Dyakonov-Perel-like Orbital and Spin Relaxations in Centrosymmetric Systems

Jeonghun Sohn, Jongjun M. Lee, and Hyun-Woo Lee[*]

Department of Physics, Pohang University of Science and Technology, Pohang 37673, Korea

The Dyakonov-Perel (DP) mechanism of spin relaxation has long been considered irrelevant in centrosymmetric systems since it was developed originally for noncentrosymmetric ones. We investigate whether this conventional understanding extends to the realm of orbital relaxation, which has recently attracted significant attention. Surprisingly, we find that orbital relaxation in centrosymmetric systems exhibits the DP-like behavior in the weak scattering regime. Moreover, the DP-like orbital relaxation can make the spin relaxation in centrosymmetric systems DP-like through the spin-orbit coupling. We also find that the DP-like orbital and spin relaxations are anisotropic even in materials with high crystal symmetry (such as face-centered cubic structure) and may depend on the orbital and spin nature of electron wave functions.

Introduction.—Electron orbital angular momentum (OAM) dynamics in solids has gotten increased attention recently [1]. Theories [2–4] predict the orbital Hall effect even in materials with strong orbital quenching and weak spin-orbit coupling (SOC). Recent experiments [5–11] verified various theoretical predictions [12–15] on the OAM. Experiments also revealed surprising stability of the OAM dynamics against disorder [7–11,16], necessitating studies on disorder effects. Disorder effects on the orbital current generation are examined theoretically [2,3,17–19]. Another urgent issue is to understand disorder effects on orbital relaxation [20].

The first primary objective of our Letter is to theoretically understand the scattering effect on orbital relaxation in centrosymmetric systems. In the case of spin, its relaxation is typically attributed to two mechanisms [21–27]. One mechanism is the Elliott-Yafet (EY) mechanism [26,27], where scattering events alter the spin direction, leading to the shorter spin relaxation time τ_s as the momentum scattering time τ_m becomes shorter ($\tau_s \propto \tau_m$). The other is the Dyakonov-Perel (DP) mechanism [23–25], where the momentum-dependent effective magnetic field (spin texture) induces the spin precession and dephasing, which is intervened by scattering. Thus, τ_s becomes *longer* as τ_m becomes shorter ($\tau_s \propto 1/\tau_m$). The momentum-dependent effective field arises from the spin-momentum coupling such as Rashba and Dresselhaus couplings, which are forbidden in centrosymmetric systems. Thus, the spin relaxation in centrosymmetric systems is commonly attributed to the EY mechanism [28–31].

Our analytic and numerical calculations show that the orbital relaxation time τ_o in centrosymmetric systems exhibits the DP-like relaxation (τ_o increases with decreasing τ_m) for sufficiently long τ_m. That is, scattering helps electrons maintain their OAM for a longer time. This is the first main result of our study. The DP-like behavior in centrosymmetric systems contradicts the common expectation that disorder scattering accelerates orbital relaxation and is also in clear contrast to the aforementioned common wisdom for spin relaxation. When τ_m is sufficiently short, we find that τ_o exhibits the EY-like relaxation (τ_o increases with increasing τ_m).

Our second primary objective is to understand spin relaxation when the SOC exists. When the spin **S** is coupled to the OAM **L**, the spin relaxation may be influenced by the orbital relaxation, raising the possibility that even spin may exhibit the DP-like relaxation behavior when τ_m is sufficiently long. Our analytic and numerical calculations confirm this possibility. This is the second main result of our study and provides a possible explanation for the DP-like spin relaxation in centrosymmetric metal Pt [32]. Our result differs from a model calculation [33], which predicts the DP spin relaxation in centrosymmetric systems when τ_m is sufficiently short.

Schematic illustration.—In centrosymmetric systems without the SOC, energy eigenstates have vanishing OAM expectation values. However, the orbital nature of the eigenstates varies with the momentum **k**. This orbital texture can induce the DP-like OAM relaxation as demonstrated below. For concreteness of illustration, we take a p orbital centrosymmetric system with three energy bands ($n = 1, 2, 3$), whose eigenstates have real orbital characters $|\chi_{n\mathbf{k}}\rangle = \hat{\mathbf{m}}_{n\mathbf{k}} \cdot \hat{\mathbf{x}}|p_x\rangle + \hat{\mathbf{m}}_{n\mathbf{k}} \cdot \hat{\mathbf{y}}|p_y\rangle + \hat{\mathbf{m}}_{n\mathbf{k}} \cdot \hat{\mathbf{z}}|p_z\rangle$ with $\hat{\mathbf{m}}_{n\mathbf{k}} \cdot \hat{\mathbf{m}}_{n'\mathbf{k}} = \delta_{n,n'}$. Here, the **k** dependence of the unit vector $\hat{\mathbf{m}}_{n\mathbf{k}}$ describes the orbital texture. For a schematically illustrated electron trajectory in Fig. 1(a), we focus on a ballistic segment from $\mathbf{r}_a$ ($a = 0, 1, 2, \cdots$) to $\mathbf{r}_{a+1}$, where the electron wave function for a given energy E may be expressed as

$$\psi_a(\mathbf{r}) = \sum_n c_{n,a} \exp{(i\mathbf{k}_{n,a} \cdot \mathbf{r})} |\chi_{n\mathbf{k}_{n,a}}\rangle. \qquad (1)$$

The n dependence of $\mathbf{k}_{n,a}$ in the exponential phase factor arises since each band component has a different wave vector for the given E. Then, the local OAM expectation value for $\psi_a(\mathbf{r})$ reduces to $\langle\mathbf{L}\rangle_{\mathbf{r}} \equiv \psi_a^\dagger(\mathbf{r})\mathbf{L}\psi_a(\mathbf{r})$ at $\mathbf{r}$, where $\mathbf{L}$ is the OAM operator. Although the OAM expectation value for each eigenstate $e^{i\mathbf{k}\cdot\mathbf{r}}|\chi_{n\mathbf{k}}\rangle$ vanishes for all $\mathbf{r}$, we emphasize that $\langle\mathbf{L}\rangle_{\mathbf{r}}$ is finite in general and varies as the electron propagates from $\mathbf{r}_a$ to $\mathbf{r}_{a+1}$. For simplicity, we take $\hat{\mathbf{m}}_{n=1,\mathbf{k}_{n=1,a}} = \hat{\mathbf{x}}$, $\hat{\mathbf{m}}_{n=2,\mathbf{k}_{n=2,a}} = \hat{\mathbf{y}}$, $\hat{\mathbf{m}}_{n=3,\mathbf{k}_{n=3,a}} = \hat{\mathbf{z}}$. Then, the three components $\langle L_x\rangle_{\mathbf{r}}$, $\langle L_y\rangle_{\mathbf{r}}$, and $\langle L_z\rangle_{\mathbf{r}}$ oscillate with the wave vectors $\mathbf{k}_{n=2,a} - \mathbf{k}_{n=3,a}$, $\mathbf{k}_{n=3,a} - \mathbf{k}_{n=1,a}$, and $\mathbf{k}_{n=1,a} - \mathbf{k}_{n=2,a}$, respectively. This illustrates that the OAM can precess intrinsically due to the orbital texture, which is allowed even in centrosymmetric systems [34].

To understand the scattering effect on the intrinsic OAM dynamics, we note that the $\langle\mathbf{L}\rangle_{\mathbf{r}}$ evolution pattern depends crucially on the eigenstate orbital characters, which vary with the propagation direction due to the orbital texture. This implies that $\langle\mathbf{L}\rangle_{\mathbf{r}}$ evolution pattern in a ballistic segment between two consecutive scatterings at $\mathbf{r}_j$ and $\mathbf{r}_{j+1}$ differs from the corresponding patterns in different ballistic segments. Therefore, each scattering alters the $\langle\mathbf{L}\rangle_{\mathbf{r}}$ evolution pattern [Fig. 1(a)], which resembles the $\langle\mathbf{S}\rangle_{\mathbf{r}}$ evolution pattern change by scattering in noncentrosymmetric systems. This implies that the DP-like OAM relaxation may occur in centrosymmetric systems.

Next, we turn on the SOC. Then, the local spin expectation value $\langle\mathbf{S}\rangle_{\mathbf{r}}$ should also evolve intrinsically since $\mathbf{S}$ is coupled to $\mathbf{L}$ and $\langle\mathbf{L}\rangle_{\mathbf{r}}$ evolves intrinsically. Moreover, $\langle\mathbf{S}\rangle_{\mathbf{r}}$
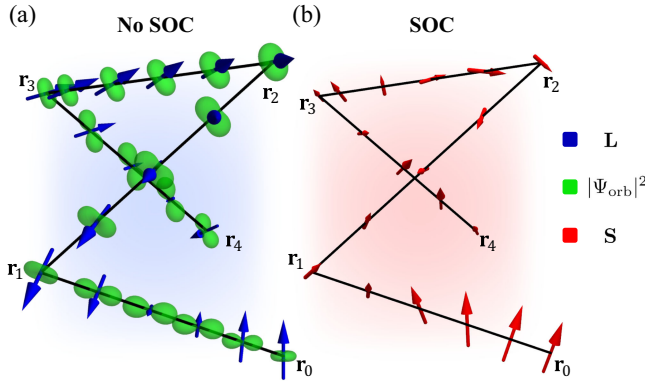

FIG. 1. Schematic illustration of the DP-like relaxation. An electron is scattered at positions $\mathbf{r}_1$, $\mathbf{r}_2$, etc., and forms a zigzag trajectory. (a) Along the trajectory, the electron's orbital density (green) and OAM (blue arrows) evolve, which results in the DP-like orbital relaxation even in centrosymmetric systems. Without the SOC, the orbital dynamics does not affect the spin dynamics. (b) When the SOC exists the spin (red arrows) dynamics is affected by the orbital dynamics. Thus the OAM in (a) can cause the spin to process, leading to the DP-like spin relaxation.

evolution pattern should change upon scattering [see the evolution of the red arrows in Fig. 1(b)] just like $\langle\mathbf{L}\rangle_{\mathbf{r}}$ does. This illustrates schematically that the DP-like spin relaxation may be possible in centrosymmetric systems when the SOC exists.

Kinetic theory approach.—To gain a more rigorous assessment of the orbital relaxation, we apply the semiclassical kinetic theory to a centrosymmetric p-orbital model system described by the Luttinger Hamiltonian [35], which was used previously to demonstrate the intrinsic orbital Hall effect in hole-doped silicon [2]. Its Hamiltonian density is given by

$$\mathcal{H}_{\mathbf{k}}^o = c_0\mathbf{k}^2 + c_1\sum_j k_j^2 L_j^2 + c_2\sum_{i\neq j}k_i k_j\{L_i, L_j\}, \quad (2)$$

where k_i and L_i denote components of $\mathbf{k}$ and $\mathbf{L}$, respectively, and $i, j = x, y, z$. Note that there is no SOC in $\mathcal{H}_{\mathbf{k}}^o$. In the first term, $\mathbf{k}$ does not couple to $\mathbf{L}$, whereas in the second and the third terms, $\mathbf{k}$ couples to $\mathbf{L}$, generating the $\mathbf{k}$-dependent variation of the real orbital character $|\chi_{n\mathbf{k}}\rangle$ (orbital texture [4]). These forms of orbital-momentum coupling do not break the inversion symmetry nor the time-reversal symmetry [35,36].

Our semiclassical kinetic theory builds upon the original work of Dyakonov and Perel [23–25], who solved the quantum Boltzmann equation and demonstrated the DP spin relaxation due to the spin texture in noncentrosymmetric systems. To assess the effect of the orbital texture on orbital relaxation in centrosymmetric systems, we treat the orbital-momentum coupling terms in $\mathcal{H}_{\mathbf{k}}^o$ as perturbations and the first term in $\mathcal{H}_{\mathbf{k}}^o$ as an unperturbed Hamiltonian. In the interaction picture, the equation of motion for the density matrix $\rho_{\mathbf{k}}$ then reads

$$\frac{\partial\rho_{\mathbf{k}}}{\partial t} = \frac{1}{i\hbar}[\mathcal{H}_{\mathbf{k}}^{om}, \rho_{\mathbf{k}}] + \left(\frac{\partial\rho_{\mathbf{k}}}{\partial t}\right)_{coll}, \quad (3)$$

where $\mathcal{H}_{\mathbf{k}}^{om}$ denotes the orbital-momentum coupling terms in Eq. (2). The commutator on the right-hand side of Eq. (3) induces the intrinsic time evolution of the orbital. The collision integral by impurities [last term in Eq. (3)] is assumed to be elastic and isotropic. Furthermore, we assume scattering-induced orbital relaxation is weak, which can be justified in the large τ_m regime, where the EY-like orbital relaxation is negligible. We investigate the evolution of the OAM, $\mathrm{Tr}[\rho_{\mathbf{k}}\mathbf{L}]$, by solving the corresponding equation and taking its angular average over the direction $\mathbf{k}$. As a result, we find the orbital relaxation time τ_o given by

$$\frac{1}{\tau_o} = f_o\tau_m, \quad (4)$$

where $f_o = (2k_F^4/15\hbar^2\gamma_o)(2c_1^2 + 3c_2^2)$, k_F is the momentum at the Fermi surface, and γ_o is a dimensionless constant

of order 1 that does not depend on τ_m [24,25,37]. Note that $1/\tau_o$ is proportional to τ_m, that is, the orbital relaxation follows the DP behavior.

Next, we introduce the SOC $\mathbf{S} \cdot \mathbf{L}$ to $\mathcal{H}_\mathbf{k}^o$ and examine the spin relaxation in a centrosymmetric p-orbital system described by

$$\mathcal{H}_\mathbf{k}^{os} = c_0 \mathbf{k}^2 + c_1 (\mathbf{k} \cdot \mathbf{L})^2 + g_{so} \mathbf{S} \cdot \mathbf{L}, \qquad (5)$$

where the third term is the SOC. The isotropic limit $(c_1 = 2c_2)$ is assumed for simplicity. With $\mathcal{H}_\mathbf{k}^{os}$, we perform a similar semiclassical calculation of the quantum Boltzmann equation. We treat the SOC as a perturbation, noting that the orbital-momentum coupling has a typical energy scale comparable with the electron hopping and is stronger than the SOC. We investigate the evolution of the spin, $\mathrm{Tr}[\rho_\mathbf{k} \mathbf{S}]$, and take its angular average over the direction $\mathbf{k}$. As a result, we find that in the large τ_m regime, the spin relaxation time τ_s is given by

$$\frac{1}{\tau_s} = f_s \tau_m, \qquad (6)$$

where $f_s = (16/3\hbar^2 \gamma_s) g_{so}^2$ and γ_s is a dimensionless constant of order 1 that does not depend on τ_m [24,25,37]. Note that $1/\tau_s$ is proportional to τ_m, that is, the spin relaxation follows the DP behavior even though the spin-momentum coupling is forbidden in this centrosymmetric system. This DP behavior is realized by the combination of the orbital texture and the SOC, as evidenced by f_s being proportional to g_{so}^2. Our results demonstrate that the orbital texture can induce the DP-like relaxation of both spin and orbital in centrosymmetric nonmagnetic systems.

Numerical calculation.—We examine the spin and orbital relaxations in centrosymmetric nonmagnetic metals (NM) numerically by using the tight-binding description. We calculate the spin-dependent or orbital-dependent *charge* conductances for a spin value [Fig. 2(a) inset] or an orbital valve [Fig. 3(a) inset], where the NM of interest is sandwiched between two spin ferromagnets (SFMs) or two orbital ferromagnets (OFMs) [46,47], which act as spin or OAM generators and detectors. We calculate the charge resistance R between the two ferromagnets (FM) for the two configurations, one with the two FMs magnetized parallel to each other (R_P) and the other with the two FMs magnetized antiparallel (R_{AP}). The resistance difference $\Delta R = R_{AP} - R_P$ amounts to the out-of-plane giant magnetoresistance, which decays as the distance d between the two FMs increases. We extract the spin and orbital relaxation lengths of the NM from the d dependence of ΔR, which changes with the disorder strength in the NM. This scheme allows one to focus on the scattering effect on longitudinal spin or orbital current relaxation in the NM and to decouple it from the scattering effect on spin [3,48] or orbital [2,3,17–19] Hall current generation in the NM
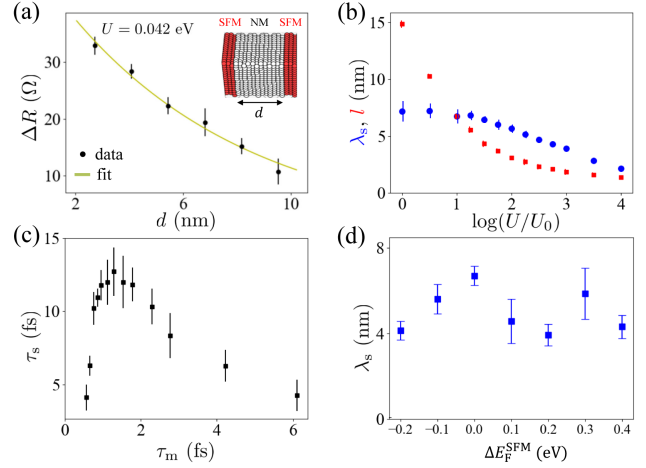

FIG. 2. Spin relaxation in NM. (a) Magnetoresistance ΔR as a function of the NM thickness d with random static disorder potential with magnitude $U = 0.042$ eV. Points denote ΔR averaged over disorder configurations. The vertical bars denote the standard deviation of ΔR. The curve denotes the exponential fitting of the points. Inset: schematic of the spin valve structure. (b) Spin relaxation length λ_s (blue) and mean free path l (red) as a function of U. (c) Spin relaxation time τ_s as a function of momentum scattering time τ_m. (d) λ_s's dependence on the on-site energy shift in SFMs.

since the latter effect does not affect ΔR. The relaxation lengths are later converted to the spin and orbital relaxation times.

Since the modeling of the SFMs is more straightforward than the OFMs, we examine the spin relaxation in a spin valve structure first [Fig. 2(a) inset]. For both the left and
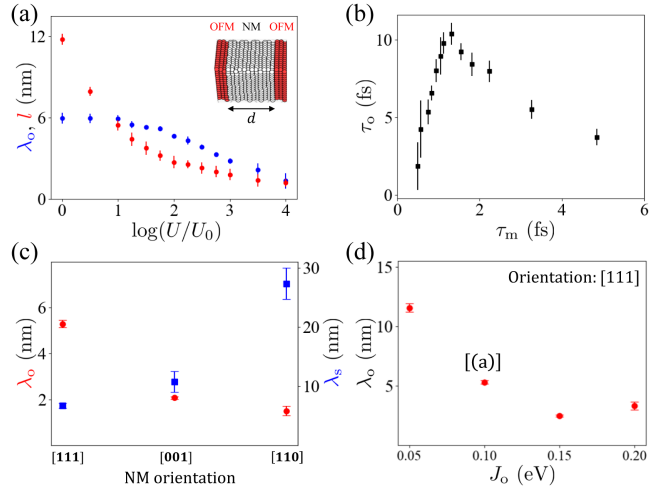

FIG. 3. Orbital relaxation in NM. (a) Orbital relaxation length λ_o (blue) and mean free path l (red) as a function of U. Inset: orbital valve structure. (b) Orbital relaxation time τ_o as a function of momentum scattering time τ_m. (c) λ_o and λ_s for several crystal directions of NM. (d) λ_o for different values of orbital exchange coupling parameter J_o. $U = 0.042$ eV in (c) and (d).

right SFMs in the spin valve, we adopt artificial FMs [37] emulating permalloy $Ni_{81}Fe_{19}$, since permalloy is commonly used to investigate spin relaxation [29,32,49]. For the NM in the spin valve, we adopt the Slater-Koster tight-binding parameters of Pt. Additionally, we introduce static on-site disorder potential with a Gaussian random distribution (mean $= 0$, standard deviation $= U$) to induce scattering in the NM. No disorder is introduced in the SFMs. All three layers in the spin valve possess the face-centered-cubic structure stacked along the [111] direction. The magnetization directions of the SFMs are perpendicular to the interfaces. Using the KWANT package [50,51], we evaluate the average (symbols) and the standard deviation (vertical bars) [Fig. 2(a)] of ΔR over the on-site disorder potential realizations, for given values of U and d. The d dependence of the average is fitted by the curve (solid line)

$$\Delta R_{\text{ave}} = \Delta R_0 e^{-d/\lambda_s}, \tag{7}$$

where λ_s is the spin relaxation length and ΔR_0 is a d-independent constant.

We then repeat the process in Fig. 2(a) for various values of U to analyze how λ_s varies with U [blue symbols in Fig. 2(b)]. The mean free path (l) is also evaluated as a function U [red symbols in Fig. 2(b)]. To determine l, we calculate the disorder-averaged resistivity of the NM [37] and convert it into l and τ_m. For $\log(U/U_0) \lesssim 2$ ($U_0 = 0.03$ eV), we find that l decays rapidly as U increases whereas λ_s decreases only mildly with U. This difference in the U dependences of l and λ_s implies that the spin relaxation time τ_s *increases* as U increases. This confirms that even in centrosymmetric systems, the DP-like spin relaxation is possible in the weak scattering regime. To quantify τ_s, we utilize the relation $\tau_s = 3\lambda_s^2 v_F^{-2} \tau_m^{-1}$ [52], where v_F is the Fermi velocity. This relation is derived in the diffusive regime ($\lambda_s \gg l$), and thus not strictly valid when λ_s is comparable to l [Fig. 2(b)]. Nevertheless, we use the relation since the diffusion picture is commonly used in the spin transport analysis even when $\lambda_s \sim l$ [32,53–55]. Figure 2(c) shows the resulting τ_s plotted as a function of τ_m. In the weak scattering regime, ($\tau_m \geq 1.5$ fs), τ_s increases with decreasing τ_m, thus exhibiting the DP-like spin relaxation. On the other hand, in the strong scattering regime ($\tau_m \leq 1.5$ fs), τ_s increases with increasing τ_m, thus exhibiting the EY-like spin relaxation.

Next, we examine orbital relaxation numerically via an orbital valve structure [Fig. 3(a) inset] with an NM sandwiched between two OFMs. All three layers in the orbital valve possess the face-centered-cubic structure stacked along the [111] direction. For the NM, we turn off the SOC in the tight-binding parameters of Pt. For the OFMs, we adopt a simple modeling of artificial OFMs instead of real OFMs [46,47]; we introduce the orbital exchange coupling $J_o\hat{\mathbf{M}} \cdot \mathbf{L}$ to the tight-binding parameters

of the NM. Here, the unit vector $\hat{\mathbf{M}}$ denotes the magnetization direction of an OFM and J_o is the strength of the orbital exchange coupling. Because of the coupling, eigenstates of the OFMs have finite OAM expectation values. The reversal of $\hat{\mathbf{M}}$ does not modify the band structure of the OFMs but reverses the OAM expectation values of eigenstates. The SOC is absent everywhere in the orbital valve so that we can focus on pure orbital relaxation dynamics, decoupled from spin dynamics. The rest of the analysis procedure is the same as the spin relaxation analysis procedure. Figure 3(a) compares the resulting orbital relaxation length λ_o and l as a function of U. Their U dependences are similar to those in Fig. 2(b). This confirms that orbital relaxation in centrosymmetric systems can exhibit the DP-like relaxation in the weak scattering regime. The relation $\tau_o = 3\lambda_o^2 v_F^{-2} \tau_m^{-1}$ is used to convert λ_o to the orbital relaxation time τ_o. The resulting τ_o is shown as a function of τ_m in Fig. 3(b), where the DP-like and EY-like orbital relaxations are evident in the weak and strong scattering regimes, respectively.

Discussions.—A few experiments [32,38,39,49] reported that the spin relaxation in centrosymmetric metallic systems exhibits the DP-like behavior in the low-temperature regime (low-resistivity regime). A recent calculation [40] also reported the DP-like spin relaxation in Pt. Since the DP spin relaxation has been believed to be forbidden in centrosymmetric systems, some [38–40] attributed the behavior to the interfaces of the centrosymmetric materials, where the inversion symmetry is broken and the spin-momentum coupling may be present. On the other hand, the experiment on Pt [32] argued that the DP spin relaxation by the interfaces is not relevant in their measurement geometry of the out-of-plane magnetoresistance [same as our spin valve geometry in Fig. 2(a) inset] and the observed DP-like behavior should originate from centrosymmetric bulk Pt. We argue that our work provides a possible explanation for the previously reported DP-like behaviors in centrosymmetric systems. To separate the interfacial and bulk contributions to the DP-like relaxation in our calculation, we turn off the SOC $\mathbf{S} \cdot \mathbf{L}$ in the bulk of the NM and retain the SOC only near the SFM/NM and the NM/SFM interfaces. A significantly longer spin relaxation length is obtained in this case [37], implying that the DP-like spin relaxation in Fig. 2 arises mainly from the bulk NM, consistent with the argument of Ref. [32]. For the orbital relaxation, on the other hand, we are not aware of any experiments that systematically examine the scattering effect. We argue that such experiments are highly needed to clarify the nature of the orbital relaxation.

Our numerical calculations reveal a couple of properties that go beyond the simple model Hamiltonians $\mathcal{H}_{\mathbf{k}}^o$ [Eq. (2)] and $\mathcal{H}_{\mathbf{k}}^{os}$ [Eq. (5)], since the Hamiltonians for the numerical calculations are more complicated. The first such property is the anisotropy of relaxation in the weak scattering regime. The anisotropy of the EY-type spin relaxation

was reported before [56,57]. To examine the relaxation anisotropy, we change the stacking direction of the spin and orbital valves from [111] to [001], and [110], and examine the out-of-plane magnetoresistance. The magnetization direction is maintained to be parallel or antiparallel to the stacking direction. We find that λ_s (λ_o) in the weak scattering regime ($U = 0.042$ eV) varies factor 4.1 (3.5) with the stacking direction [Fig. 3(c)]. We attribute the relaxation anisotropy to the inequality $\lambda_s, \lambda_o \lesssim l$ [Figs. 2(b) and 3(a)], frequently encountered situations in experiments [5,10,30,58,59]. In such situations, electron properties are not averaged over the entire Fermi surface but instead influenced strongly by relatively narrow regions of the Fermi surface that vary with the electron propagation direction. Interestingly, the [111] ([110]) direction has the smallest (largest) λ_s but the largest (smallest) λ_o. We attribute this behavior to the direction-dependent orbital environment change. Along the [111] direction, the C_3 rotational symmetry safeguards the twofold orbital degeneracy of d_{xy} and $d_{x^2-y^2}$ character states [60] (z along [111]), facilitating the transport of $L_z = \pm 2\hbar$ orbital ($d_{x^2-y^2} \pm i d_{xy}$) and resulting in the longest λ_o. The importance of the degeneracy for λ_o was reported for NM [61] and FM [62]. In such a situation with orbital degeneracy, the SOC becomes more effective and can modify the eigenstates significantly (thereby suppressing λ_s). Exactly opposites apply to the [110] direction, along which a large crystal field splitting occurs. In such a situation with the lifted orbital degeneracy, the SOC becomes ineffective (thereby enhancing λ_s). The relaxation anisotropy also raises a possibility that for a given multilayer structure with a well-defined stacking direction, its out-of-plane transport [32,59] and lateral transport [49,63] may have different relaxation length scales [52]. A recent calculation on Pt [40] reported that the spin relaxation lengths along the transverse and longitudinal directions are different from each other, although its relation with our result [Fig. 3(c)] is unclear. Further study is needed to clarify the relaxation anisotropy, which is in clear contrast to the spin (orbital) Hall conductivity that is isotropic in the face-centered-cubic materials.

Also, we find that λ_o and λ_s depend not only on the material parameters of NMs but also on those of OFMs and SFMs. Figure 3(d) shows the variation of λ_o as the orbital exchange coupling parameter J_o changes, and Fig. 2(d) shows the variation of λ_s with ΔE_F^{SFM}, where ΔE_F^{SFM} denotes the on-site energy shift of all sites in SFMs. Both figures are obtained in the weak scattering regime ($U = 0.042$ eV). Considering that J_o and ΔE_F^{SFM} modify the wave function shape of the states at the Fermi energy of OFMs and SFMs, respectively, we attribute the J_o- and ΔE_F^{SFM} dependences to the λ_o and λ_s dependences on the wave function nature of injected electrons when $\lambda_o, \lambda_s \lesssim l$. This result may provide a partial explanation as to why diverse values of λ_s are obtained for the same NMs in experiments [52,58,64] since λ_s may vary with FMs in contact with NMs.

An important outstanding problem is to resolve the discrepancy between experiments reporting long λ_o (ranging from several nanometers [5,16] to tens of nanometers [7,8,16]) and calculations reporting much shorter λ_o (typically less than one nanometer [20,40,61,65]). Although our calculation cannot resolve the discrepancy since it aims to explore qualitative behaviors of λ_o and τ_o instead of their quantitative accuracy, the anisotropy [Fig. 3(c)] and the FM dependence [Fig. 3(d)] of λ_o may be of relevance to the discrepancy. Another outstanding problem, which may be related to the above problem, is to understand orbital relaxation in polycrystalline systems. Most experiments on orbital transport utilize polycrystalline materials [7–11,16], whereas polycrystallinity is ignored in all existing calculations. It was suggested [66] that orbital transport may be more efficient in polycrystalline materials than in single crystals. A recent experiment [16] supports this suggestion. Further studies are needed for these outstanding problems.

Conclusion.—We demonstrated that in the weak scattering regime, both orbital and spin relaxations may exhibit DP-like behaviors even in centrosymmetric systems. The orbital texture plays a crucial role in the DP-like relaxations. Our results provide an explanation for a recent experiment on DP-like spin relaxation in Pt [32] and predict the relaxation anisotropy and relaxation's dependence on the orbital and spin nature of electron wave functions. More experiments are needed to investigate intriguing properties of orbital and spin relaxations systematically.

J. S. and J. M. L. contributed equally to this letter.

*Corresponding author: hwl@postech.ac.kr

[1] D. Go, D. Jo, H.-W. Lee, M. Kläui, and Y. Mokrousov, Orbitronics: Orbital currents in solids, Europhys. Lett. **135**, 37001 (2021).

[2] B. A. Bernevig, T. L. Hughes, and S. C. Zhang, Orbitronics: The intrinsic orbital current in p-doped silicon, Phys. Rev. Lett. **95**, 066601 (2005).

[3] T. Tanaka, H. Kontani, M. Naito, T. Naito, D. S. Hirashima, K. Yamada, and J. Inoue, Intrinsic spin Hall effect and orbital Hall effect in 4d and 5d transition metals, Phys. Rev. B **77**, 165117 (2008).

[4] D. Go, D. Jo, C. Kim, and H. W. Lee, Intrinsic spin and orbital Hall effects from orbital texture, Phys. Rev. Lett. **121**, 086602 (2018).

[5] S. Lee, M. G. Kang, D. Go, D. Kim, J. H. Kang, T. Lee, G. H. Lee, J. Kang, N. J. Lee, Y. Mokrousov, S. Kim,

K. J. Kim, K. J. Lee, and B. G. Park, Efficient conversion of orbital Hall current to spin current for spin-orbit torque switching, Commun. Phys. **4**, 234 (2021).

[6] D. Lee, D. Go, H.-J. Park, W. Jeong, H.-W. Ko, D. Yun, D. Jo, S. Lee, G. Go, J. H. Oh, K.-J. Kim, B.-G. Park, B.-C. Min, H. C. Koo, H.-W. Lee, O. Lee, and K.-J. Lee, Orbital torque in magnetic bilayers, Nat. Commun. **12**, 6710 (2021).

[7] Y.-G. Choi, D. Jo, K.-H. Ko, D. Go, K.-H. Kim, H. G. Park, C. Kim, B.-C. Min, G.-M. Choi, and H.-W. Lee, Observation of the orbital Hall effect in a light metal Ti, Nature (London) **619**, 52 (2023).

[8] H. Hayashi, D. Jo, D. Go, T. Gao, S. Haku, Y. Mokrousov, H. W. Lee, and K. Ando, Observation of long-range orbital transport and giant orbital torque, Commun. Phys. **6**, 32 (2023).

[9] G. Sala, H. Wang, W. Legrand, and P. Gambardella, Orbital hanle magnetoresistance in a 3d transition metal, Phys. Rev. Lett. **131**, 156703 (2023).

[10] I. Lyalin, S. Alikhah, M. Berritta, P. M. Oppeneer, and R. K. Kawakami, Magneto-optical detection of the orbital Hall effect in chromium, Phys. Rev. Lett. **131**, 156702 (2023).

[11] T. S. Seifert, D. Go, H. Hayashi, R. Rouzegar, F. Freimuth, K. Ando, Y. Mokrousov, and T. Kampfrath, Time-domain observation of ballistic orbital-angular-momentum currents with giant relaxation length in tungsten, Nat. Nanotechnol. **18**, 1132 (2023).

[12] D. Jo, D. Go, and H.-W. Lee, Gigantic intrinsic orbital Hall effects in weakly spin-orbit coupled metals, Phys. Rev. B **98**, 214405 (2018).

[13] L. Salemi and P. M. Oppeneer, First-principles theory of intrinsic spin and orbital Hall and nernst effects in metallic monoatomic crystals, Phys. Rev. Mater. **6**, 095001 (2022).

[14] D. Go and H. W. Lee, Orbital torque: Torque generation by orbital current injection, Phys. Rev. Res. **2**, 013177 (2020).

[15] D. Go, F. Freimuth, J.-P. Hanke, F. Xue, O. Gomonay, K.-J. Lee, S. Blügel, P. M. Haney, H.-W. Lee, and Y. Mokrousov, Theory of current-induced angular momentum transfer dynamics in spin-orbit coupled systems, Phys. Rev. Res. **2**, 033401 (2020).

[16] J. C. Idrobo, J. Rusz, G. Datt, D. Jo, S. Alikhah, D. Muradas, U. Noumbe, M. V. Kamalakar, and P. M. Oppeneer, Direct observation of nanometer-scale orbital angular momentum accumulation, arXiv:2403.09269.

[17] P. Tang and G. E. W. Bauer, Role of disorder in the intrinsic orbital Hall effect, arXiv:2401.17620.

[18] H. Liu and D. Culcer, Dominance of extrinsic scattering mechanisms in the orbital Hall effect: Graphene, transition metal dichalcogenides and topological antiferromagnets, arXiv:2308.14878.

[19] L. M. Canonico, J. H. García, and S. Roche, Real-space calculation of orbital Hall responses in disordered materials, arXiv:2404.01739.

[20] M. Rang and P. J. Kelly, Orbital relaxation length from first-principles scattering calculations, arXiv:2403.06827.

[21] I. Žutić, J. Fabian, and S. D. Sarma, Spintronics: Fundamentals and applications, Rev. Mod. Phys. **76**, 323 (2004).

[22] M. W. Wu, J. H. Jiang, and M. Q. Weng, Spin dynamics in semiconductors, Phys. Rep. **493**, 61 (2010).

[23] M. I. Dyakonov and V. I. Perel, Spin relaxation of conduction electrons in noncentrosymmetric semiconductors, Sov. Phys. Solid State, USSR **13**, 3023 (1972).

[24] M. I. Dyakonov and V. I. Perel, Theory of optical spin orientation of electrons and nuclei in semiconductors, Opt. Orientat. **8**, 11 (1984).

[25] J. Fabian, A. Matos-Abiague, C. Ertler, P. Stano, and I. Žutić, Semiconductor spintronics, Acta Phys. Slovaca **57**, 565 (2007).

[26] R. J. Elliott, Theory of the effect of spin-orbit coupling on magnetic resonance in some semiconductors, Phys. Rev. **96**, 266 (1954).

[27] Y. Yafet, g factors and spin-lattice relaxation of conduction electrons, Solid State Phys. **14**, 1 (1963).

[28] Y. Niimi, D. Wei, H. Idzuchi, T. Wakamura, T. Kato, and Y. C. Otani, Experimental verification of comparability between spin-orbit and spin-diffusion lengths, Phys. Rev. Lett. **110**, 016805 (2013).

[29] E. Sagasta, Y. Omori, M. Isasa, M. Gradhand, L. E. Hueso, Y. Niimi, Y. C. Otani, and F. Casanova, Tuning the spin Hall effect of Pt from the moderately dirty to the superclean regime, Phys. Rev. B **94**, 060412(R) (2016).

[30] M. H. Nguyen, D. C. Ralph, and R. A. Buhrman, Spin torque study of the spin Hall conductivity and spin diffusion length in platinum thin films with varying resistivity, Phys. Rev. Lett. **116**, 126601 (2016).

[31] H. Y. Nguyen, W. P. Pratt, and J. Bass, Spin-flipping in Pt and at Co/Pt interfaces, J. Magn. Magn. Mater. **361**, 30 (2014).

[32] R. Freeman, A. Zholud, Z. Dun, H. Zhou, and S. Urazhdin, Evidence for Dyakonov-Perel-like spin relaxation in Pt, Phys. Rev. Lett. **120**, 067204 (2018).

[33] P. Boross, B. Dóra, A. Kiss, and F. Simon, A unified theory of spin-relaxation due to spin-orbit coupling in metals and semiconductors, Sci. Rep. **3**, 1 (2013).

[34] S. Han, H. W. Lee, and K. W. Kim, Microscopic study of orbital textures, Curr. Appl. Phys. **50**, 13 (2023).

[35] J. M. Luttinger, Quantum theory of cyclotron resonance in semiconductors: General theory, Phys. Rev. **102**, 1030 (1956).

[36] S. Han, H. W. Lee, and K. W. Kim, Orbital dynamics in centrosymmetric systems, Phys. Rev. Lett. **128**, 176601 (2022).

[37] See Supplemental Material at http://link.aps.org/supplemental/10.1103/PhysRevLett.132.246301 for further details, which include Refs. [24,25,29,32,34,35,38–45].

[38] G. Mihajlović, J. E. Pearson, S. D. Bader, and A. Hoffmann, Surface spin flip probability of mesoscopic Ag wires, Phys. Rev. Lett. **104**, 237202 (2010).

[39] J. Ryu, M. Kohda, and J. Nitta, Observation of the D'yakonov-Perel' spin relaxation in single-crystalline Pt thin films, Phys. Rev. Lett. **116**, 256802 (2016).

[40] K. D. Belashchenko, G. G. Baez Flores, W. Fang, A. A. Kovalev, M. van Schilfgaarde, P. M. Haney, and M. D. Stiles, Breakdown of the drift-diffusion model for transverse spin transport in a disordered Pt film, Phys. Rev. B **108**, 144433 (2023).

[41] M. D. Mower, G. Vignale, and I. V. Tokatly, Dyakonov-Perel spin relaxation for degenerate electrons in the electron-hole liquid, Phys. Rev. B **83**, 155205 (2011).

[42] P. Yu, X. F. Jin, J. Kudrnovský, D. S. Wang, and P. Bruno, Curie temperatures of fcc and bcc nickel and permalloy: Supercell and Green's function methods, Phys. Rev. B **77,** 054431 (2008).

[43] D. A. Papaconstantopoulos, *Handbook of the Band Structure of Elemental Solids: From Z =1 To Z = 112,* 2nd ed. (Springer, New York, 2015), p. 1.

[44] P. E. Lindelof and S. Wang, Bulk and surface spin-orbit relaxation of the conduction electrons separated by weak-localization experiments, Phys. Rev. B **33,** 1478 (1986).

[45] J. Q. Wang and G. Xiao, Large finite-size effect of giant magnetoresistance in magnetic granular thin films, Phys. Rev. B **51,** 5863 (1995).

[46] C. L. Tschirhart, M. Serlin, H. Polshyn, A. Shragai, Z. Xia, J. Zhu, Y. Zhang, K. Watanabe, T. Taniguchi, M. E. Huber, and A. F. Young, Imaging orbital ferromagnetism in a moiré Chern insulator, Science **372,** 1323 (2021).

[47] R. Shindou and N. Nagaosa, Orbital ferromagnetism and anomalous Hall effect in antiferromagnets on the distorted fcc lattice, Phys. Rev. Lett. **87,** 116801 (2001).

[48] S. Murakami, Absence of vertex correction for the spin Hall effect in p-type semiconductors, Phys. Rev. B **69,** 241202(R) (2004).

[49] T. Kimura, T. Sato, and Y. Otani, Temperature evolution of spin relaxation in a NiFe/Cu lateral spin valve, Phys. Rev. Lett. **100,** 066602 (2008).

[50] C. W. Groth, M. Wimmer, A. R. Akhmerov, and X. Waintal, KWANT: A software package for quantum transport, New J. Phys. **16,** 063065 (2014).

[51] P. R. Amestoy, I. S. Duff, J. Y. L'Excellent, and J. Koster, A fully asynchronous multifrontal solver using distributed dynamic scheduling, SIAM J. Matrix Anal. Appl. **23,** 15 (2006).

[52] J. Bass and W. P. Pratt, Spin-diffusion lengths in metals and alloys, and spin-flipping at metal/metal interfaces: An experimentalist's critical review, J. Phys. Condens. Matter **19,** 183201 (2007).

[53] Q. Yang, P. Holody, S.-F. Lee, L. L. Henry, R. Loloee, P. A. Schroeder, W. P. Pratt, and J. Bass, Spin flip diffusion length and giant magnetoresistance at low temperatures, Phys. Rev. Lett. **72,** 3274 (1994).

[54] J. Bass, Q. Yang, S. F. Lee, P. Holody, R. Loloee, P. A. Schroeder, and J. Pratt, W. P., How to isolate effects of spin-flip scattering on giant magnetoresistance in magnetic multilayers (invited), J. Appl. Phys. **75,** 6699 (1994).

[55] A. Fert, J.-L. Duvail, and T. Valet, Spin relaxation effects in the perpendicular magnetoresistance of magnetic multilayers, Phys. Rev. B **52,** 6513 (1995).

[56] B. Zimmermann, P. Mavropoulos, S. Heers, N. H. Long, S. Blügel, and Y. Mokrousov, Anisotropy of spin relaxation in metals, Phys. Rev. Lett. **109,** 236603 (2012).

[57] B. Zimmermann, P. Mavropoulos, N. H. Long, C.-R. Gerhorst, S. Blügel, and Y. Mokrousov, Fermi surfaces, spin-mixing parameter, and colossal anisotropy of spin relaxation in transition metals from *ab initio* theory, Phys. Rev. B **93,** 144403 (2016).

[58] J. C. Rojas-Sánchez, N. Reyren, P. Laczkowski, W. Savero, J. P. Attané, C. Deranlot, M. Jamet, J. M. George, L. Vila, and H. Jaffrès, Spin pumping and inverse spin Hall effect in platinum: The essential role of spin-memory loss at metallic interfaces, Phys. Rev. Lett. **112,** 106602 (2014).

[59] H. Kurt, R. Loloee, K. Eid, W. P. Pratt, and J. Bass, Spin-memory loss at 4.2 K in sputtered Pd and Pt and at Pd/Cu and Pt/Cu interfaces, Appl. Phys. Lett. **81,** 4787 (2002).

[60] L. Fu, Topological crystalline insulators, Phys. Rev. Lett. **106,** 106802 (2011).

[61] S. Urazhdin, Symmetry constraints on orbital transport in solids, Phys. Rev. B **108,** L180404 (2023).

[62] D. Go, D. Jo, K.-W. Kim, S. Lee, M.-G. Kang, B.-G. Park, S. Blügel, H.-W. Lee, and Y. Mokrousov, Long-range orbital torque by momentum-space hotspots, Phys. Rev. Lett. **130,** 246701 (2023).

[63] S. O. Valenzuela and M. Tinkham, Direct electronic measurement of the spin Hall effect, Nature (London) **442,** 176 (2006).

[64] X. Tao, Q. Liu, B. Miao, R. Yu, Z. Feng, L. Sun, B. You, J. Du, K. Chen, S. Zhang *et al.*, Self-consistent determination of spin Hall angle and spin diffusion length in Pt and Pd: The role of the interface spin loss, Sci. Adv. **4,** eaat1670 (2018).

[65] L. Salemi, M. Berritta, and P. M. Oppeneer, Quantitative comparison of electrically induced spin and orbital polarizations in heavy-metal/3d-metal bilayers, Phys. Rev. Mater. **5,** 074407 (2021).

[66] L. Liao, F. Xue, L. Han, J. Kim, R. Zhang, L. Li, J. Liu, X. Kou, C. Song, F. Pan, and Y. C. Otani, Efficient orbital torque in polycrystalline ferromagnetic-metal/Ru/Al_2O_3 stacks: Theory and experiment, Phys. Rev. B **105,** 104434 (2022).